First Principles Modelling of Interstitial Aggregates in Germanium

Stefan Birner

submitted by Stefan Birner to the University of Exeter as a thesis for the degree of Master of Physics with European Study in the School of Physics.

Declaration

I hereby declare that this thesis has not been submitted, either in the same or different form, to this or any other University for a degree.

Stefan Birner

May 2000

F302 Master of Physics

Physics with European Study

First Principles Modelling of Interstitial Aggregates in Germanium

PHY4419 Project and Dissertation

Final Dissertation

Stefan Birner

stefan.birner@gmx.de

Abstract

Silicon-germanium alloys are attracting great interest from the point of view of device manufacture, but to date relatively little research has been performed regarding point defects that can lead to deterioration of the electrical characteristics for this material. Native defects in silicon are known to introduce carrier traps, and one can draw some conclusions from the properties of these defects in the pure materials. However, the picture for germanium is less well developed, especially with respect to detailed microscopic models.

In this thesis the results of *ab initio* cluster calculations (local spin density functional theory) regarding the low energy structures of the isolated germanium interstitial I_1 and its aggregates I_2, I_3 and I_4 are presented. For each defect several geometries are considered. The energetically favourable structures are compared with silicon, and the properties of the low energy structures are calculated and compared with experiment. The energetics of the defects investigated here are broadly similar to the results found for the corresponding defects in Si but quite different from diamond. As with silicon, the single interstitial is found to be lowest in energy in the $\langle 110 \rangle$-oriented split-interstitial configuration. Aggregates of two and three interstitials consist of arrangements of three and four atoms sharing a single lattice site respectively, whereas the case of four interstitials has lowest energy when arranged in the $\langle 100 \rangle$-oriented configuration also found for silicon and diamond. The results on the relative energies for different configurations as well as the electrical levels for each case are presented.

Acknowledgement

I would like to thank my supervisors Prof. Dr. Bob Jones and Dr. Jonathan Goss for their guidance during this MPhys project. Especially Jonathan Goss supported me a lot and never got tired of answering all my questions. Many thanks also to James Coomer for very useful discussions and to Dr. Sven Öberg for carrying out many calculations. I also would like to thank all the members of the AIMPRO group for such an interesting and enjoyable year and for lots of hints while tackling various problems, namely Dr. John Rowe, José Coutinho, Dr. Christopher Latham, Dr. Caspar Fall, Dr. Markus Kaukonen and Ben Houraine. Thanks to Dr. Rainer Sielemann from the Hahn-Meitner-Institut in Berlin for fruitful discussions.

I would like to shout a big thank to my lovely flat mates in Lafrowda A4, Ainhoa, Cristina, Donall, Florent, Itxaso, Kélig, Lee, Maureen, Michal, Pepe, René and Simon who made this year really enjoyable and made me feel very happy after spending lots of evenings in the lab on the 2nd floor. Thanks to my parents Richard and Barbara for supporting my stay in England and my brother Matthias for sorting out lots of things while I was away from home.

Finally, I would like to thank my special Barbara for being the main source of my motivation throughout this year.

Contents

1 Introduction **10**

2 Theoretical method **13**

2.1 The AIMPRO approach 13

2.2 Calculation of donor and acceptor levels 17

3 Self-interstitials **18**

3.1 Models for the single interstitial 18

3.2 The self-interstitial and its aggregates in diamond and silicon 21

3.2.1 Single interstitial I_1 21

3.2.2 Di-interstitial I_2 22

3.2.3 Tri-interstitial I_3 23

3.2.4 Tetra-interstitial I_4 24

3.3 The self-interstitial and its aggregates in germanium 26

3.3.1 Ge single interstitial I_1 26

3.3.2 Ge di-interstitial I_2 31

3.3.3 Ge tri-interstitial I_3 33

3.3.4 Ge tetra-interstitial I_4 35

4 Conclusions **37**

5 References **39**

List of Publications, Poster Presentations and Oral Presentations

- Publication

  Theory of interstitial aggregates in germanium

  S. Birner, J.P. Goss, R. Jones, P.R. Briddon, S. Öberg, submitted to ENDEASD Workshop 2000 Proceedings, Stockholm, June 2000

- Poster Presentation

  Theory of interstitial aggregates in germanium

  S. Birner, J.P. Goss, R. Jones, P.R. Briddon, S. Öberg, ENDEASD Workshop 2000, Stockholm, 27/06/2000

- Oral Presentations

  Interstitial aggregates in germanium

  - Physik Department, Technische Universität München, Garching, 18/04/2000
  - Institut für Physik, Universität Augsburg, Augsburg, 11/04/2000
  - Institut für Physikalische und Theoretische Chemie, Technische Universität München, Garching, 06/04/2000
  - AIMPRO Workshop - Defects in Semiconductors, Exeter, 11/01/2000

List of Figures

1 The bond centred interstitial 18
2 The hexagonal interstitial 19
3 Left: Cluster containing a tetrahedral interstitial. Right: The interstitial is placed into a tetrahedral cage. 19
4 Unit cell and $\langle 100 \rangle$ split-interstitial [16] 20
5 The $\langle 110 \rangle$ split-interstitial 20
6 The NN di-interstitial in diamond 22
7 The C_{1h} di-interstitial model for Si proposed by Kim. 22
8 The C_{1h} di-interstitial model for Si found by Coomer. 23
9 The tri-interstitial model responsible for the O3 centre in diamond. 23
10 The tri-interstitial model proposed for the W-optical centre in Si. 24
11 The tetra-interstitial model proposed by Arai for Si. 25
12 The relaxed $\langle 110 \rangle$ split-interstitial configuration in Ge obtained with the AIMPRO cluster code. The fivefold-coordinated atoms are indicated by the letter B, the dimer atoms by A. . 27
13 The C_{1h} model which is a distorted $\langle 100 \rangle$ split-interstitial. . . 28
14 The Kohn-Sham levels of the lowest I_1 structures in the neutral, 1+ and 2+ charge states. The filled (unfilled) boxes represent occupied (unoccupied) states. 30
15 The C_2 di-interstitial model which is very similar to the model found by Coomer. Its C_2 axis is along the [110] direction. . . 31
16 The C_i di-interstitial model which is very similar to the model responsible for the EPR R1 centre in diamond. 32
17 The Kohn-Sham levels of the lowest energy I_2 structures. The model similar to the R1 centre in diamond clearly shows empty states in the band gap due to its under-coordination. . 33

18 The tri-interstitial model proposed by Colombo for Si. 34
19 The tri-interstitial model proposed be Gharaibeh *et al.* for Si. 34
20 In Ge the I_3 has empty states in the band gap. 36
21 In Ge the band gap has a singlet and a doublet level for the I_4. 37

List of Tables

1 Acceptor and donor energies of Au [13] and Se [15] are given in eV relative to the valence or conduction band edge. 18

2 The centres in diamond and silicon identified with I_n. 25

3 A comparison of the bond lengths (in Å) and their ratios in Ge and Si obtained with cluster (AIMPRO) and super-cell codes (da Silva, Clark). 27

4 Total energies of the I_1 in the neutral, 1+ and 2+ charge states. Brackets indicate that the defect was only stable when symmetry constrained, 'sc' stands for super-cell calculation where the highest possible point group symmetry was used. These defects could be unstable when no symmetry constraints are applied. 30

5 Total energies of I_3 in the 300 atom cluster (atom centred). . 35

6 Total energies of I_3 in the 307 atom cluster (tetrahedral interstitial site centred). 35

1 Introduction

Interstitials are extra atoms that are positioned between or sharing normal lattice sites. Native interstitials that arise from the lattice itself are called self-interstitials. They can be created by irradiating the sample with electrons, neutrons, protons or ions with sufficient energy which can lead to the formation of extended defects, depending on energy, dose and annealing temperature. These extended defects can then be associated with interstitial emission.

Self-interstitials in group IV materials and the processes by which they aggregate have attracted a lot of attention in recent years for various reasons. It is likely that future electronics devices will be based on SiGe alloys because they offer very good prospects regarding band gap engineering with the purpose of increasing device efficiency. Epitaxial growth of high quality Ge on Si substrates is hindered by a 4.2 % lattice mismatch. Nevertheless, efficient high-speed near-infrared Ge photo-detectors integrated on Si substrates demonstrate a dramatic enhancement of the performance compared to ordinary devices [1]. The understanding of the structure of defects in pure Si and Ge and their properties is therefore very important from the point of view of device manufacture when it comes to more complex alloys.

Both Si and Ge grow in the highly symmetric diamond structure, have four valence electrons outside closed shells and a similar lattice constant. The lattice ions have tetrahedral symmetry and are fourfold-coordinated. C, Si and Ge can have a different coordination number under certain circumstances, *e.g.* in defect configurations or in graphite which is another solid phase of carbon. It is more favourable for Si and Ge atoms to be fivefold-coordinated rather than threefold-coordinated. However, carbon prefers threefold-coordination to over-coordination. Therefore it is no surprise that diamond defect geometries differ from Si and Ge ones. Unlike diamond, the existence of self-interstitial atoms in silicon and germanium

has unambiguously been confirmed in experiment only when they take the shape of extended clusters or complex with impurities. Furthermore, {001}-platelets in diamond are also believed to be interstitial related. In order to understand the mechanism of forming extended defects one needs to understand the nature of the basic building blocks like small aggregates of interstitials. In diamond, these small aggregates are well understood.

Self-interstitial atoms and their complexes may cause active energy levels inside the band gap or optical centres but it is very difficult to assign signals in detected spectra to them. For extended clusters, this assignment is easier. Electron spin resonance (ESR), often called electron paramagnetic resonance (EPR), measures the transition between two states of unpaired electrons induced by incident microwaves. Defects containing unpaired electrons are called paramagnetic. EPR studies of interstitials in Si and Ge samples fail in producing comparably good results that are achieved with vacancies and their complexes [2]. There are technical difficulties in interpreting EPR experiments for Ge, which occurs in five isotopes with similar abundances. Nevertheless, recent EPR experiments have pointed out that the so-called R1 centre in diamond is due to a di-interstitial [3], the O3 centre [4] is due to a tri-interstitial and the R2 centre is a $\langle 100 \rangle$-oriented split-interstitial [5].

Although many investigations in silicon both theoretically and experimentally, e.g. using high-resolution transmission electron spectroscopy (HRTEM) [6] have been performed, there is very little known about the small aggregates and the energetics of the extended {001}- and {311}-oriented defects in germanium. Only the hydrogenated self-interstitial has been identified [7]. However, recent experiments may have provided some new microscopic information about the single interstitial [8]. In Si there is evidence that the structure of small self-interstitial aggregates is very different from that of extended {311} defects.

It is believed that the self-interstitial in Si which is emitted from extended defects during annealing processes after ion implantation is responsible for

the boron transient enhanced diffusion (TED). However, even when there are no extended defects, TED is present, suggesting that small aggregates of interstitials exist. Boron TED limits the size of next-generation sub-micron semiconductor devices, therefore it is important to understand these microscopic processes and a theory of interstitials in all group IV materials is highly desirable.

The aim of this work is to investigate the self-interstitial in germanium and small aggregates of it, namely the di-interstitial I_2, tri-interstitial I_3 and the tetra-interstitial I_4. Different geometries for the self-interstitial and its aggregates are considered using various models already proposed for diamond and silicon. The defects are enclosed in a hydrogen-terminated germanium cluster consisting of from 132 to 308 atoms. The clusters are then relaxed by means of *ab initio* (from first principles) simulations using the local density functional (LDF) real space cluster code AIMPRO [9] (*Ab initio* modelling program) which was developed in Exeter and Newcastle. The structural and electrical properties are compared with the structures and energies for the models in the literature for silicon, and the electronic levels that the lowest energy structures possess are examined in more detail.

2 Theoretical method

2.1 The AIMPRO approach

Density functional theory simplifies the computational effort of the many-body problem by using the charge density to describe the system rather than calculating the wave function for each electron explicitly. The non-relativistic many-body Schrödinger equation involves both the electrons and the ions, and the Hamiltonian H contains the kinetic energy of the ions T_i, the kinetic energy of the electrons T_e, the ion-ion potential energy V_{i-i}, the interaction energy between electrons and ions V_{e-i}, and the interaction between the electrons V_{e-e}. The wave function Ψ depends on the positions $\mathbf{r}$ and the spins s of the electrons, E is the energy.

$$(H - E)\Psi(\mathbf{r}, s) = (T_i + T_e + V_{i-i} + V_{e-i} + V_{e-e} - E)\,\Psi(\mathbf{r}, s) = 0$$

The final structure of the cluster and its properties are derived from first principles, i.e. no empirical data is needed because everything is contained in the solution of this Hamiltonian. To find the solution of this equation several approximations have to be made.

- Firstly, the motion of the electrons is treated independently of the motion of the ions. This is justified by the fact that the ions are very much heavier than the electrons and therefore their dynamical behaviour only modulates the wave functions of the electrons (Born-Oppenheimer approximation). The solution of this equation, the structural potential energy, gives the positions of the nuclei.

- Secondly, the electron-electron interaction potential V_{e-e} is described as an effective one-body potential in which the electrons move independently. The Schrödinger equation then becomes separable and the problem is solved. This effective potential consists of two terms, the exchange-correlation potential V_{XC} and the Hartree potential which

is the electrostatic potential due to the electron density. Density functional theory determines V_{XC} only by the electron spin density. Unfortunately, this quantity is known only for the homogeneous electron gas and local density functional (LDF) theory makes use of the function obtained from the homogeneous electron gas (LDA = local density approximation).

- Thirdly, only valence electrons need to be considered. Thus pseudo-potentials due to Bachelet, Hamann and Schlüter (BHS) [10] are used in order to neglect the core electrons which do not contribute to bonding.

Hohenberg and Kohn [11] showed that there is a 1:1 correspondence between the non-degenerate ground state wave function $\Psi(\mathbf{r})$ and the electron density n. The potential V_{e-i} is also uniquely determined by the electron density. This is remarkable because the energy E is then a function of the density n which depends only on three spatial variables (in the absence of spin) instead of depending on $3m$ variables when having a system of m electrons, which would inevitably lead to problems when treating large systems. Still, the remaining eigenvalue problem needs to be solved:

$$H\Psi_\lambda(\mathbf{r}, s) = E\Psi_\lambda(\mathbf{r}, s)$$

H includes the kinetic energy, the sum of the pseudo-potentials for all ions and the effective potential depending on the density of the electrons. The wave function can be written as a space dependent term multiplied by a spin function $\chi(s)$. The spatial part is expanded in terms of a basis $\phi_i(\mathbf{r})$.

$$\Psi_\lambda(\mathbf{r}, s) = \chi_\lambda(s) \sum_i c_i^\lambda \phi_i(\mathbf{r})$$

Instead of using plane waves for ϕ, AIMPRO uses Cartesian Gaussian orbitals of the form

$$x^{n_1} y^{n_2} z^{n_3} \exp(-ar^2)$$

when centred at the origin. Normally, they are centred at the nuclei and sometimes between the nuclei at bond centred sites. s Gaussian orbitals are spherically symmetric functions. This is achieved by choosing $n_i = 0$ for all $i = 1, 2, 3$. p orbitals are created by choosing $n_i = 1$ (for one i) and for the other two i's zero. All integrals that appear for Gaussian orbitals can be solved analytically. Finally the output spin density can be obtained which needs to be made consistent with the input spin density used to generate the effective potential in a self-consistent cycle. The resulting self-consistent spin density yields the structural potential energy which is used to calculate the forces on each atom. The atoms are moved via a conjugate gradient algorithm until these forces vanish in the relaxation process of the cluster. The clusters, which are hydrogen terminated to remove any surface states, are usually chosen to be either atom centred, bond centred or centred at the tetrahedral or hexagonal interstitial sites according to the point symmetry group of the defect, i.e. for a single interstitial in a tetrahedral cage (Fig. 3), the tetrahedral interstitial site centred cluster is ideal. For larger defects (I_3, I_4) bigger clusters are needed to minimise defect-surface interactions which are a disadvantage of the cluster method.

AIMPRO makes use of two different basis sets (set of Gaussian functions). The first one is used to describe the wave functions, the other one describes the charge density. Bond centred Gaussian fitting functions (s orbitals) are placed between two atoms to model the charge distribution in a bond centre, i.e. where the valence charge is localised in the cluster. Thus one Ge atom has four bond centres that connect it to nearest neighbours. For each bond centre a set of s and p functions is added to the wave function basis. Placing additional atoms (interstitials) into the cluster will change the arrangement and the number of bond centres. One has to be careful when placing these bond centres because these fitting functions will locally improve the wave function and charge density modelling, and therefore affect the total energy. When comparing the total energies of different

configurations of interstitial aggregates one has to use the same number of bond centres although each defect might have its own 'ideal' number of bond centres. When adding or removing bond centres one has to consider that the arrangement of the bond centres reflects the symmetry of the defect since otherwise energy levels or local vibrational modes might not posses the required degeneracy. Different starting arrangements of bond centres may lead to different resulting structures when the starting structure is unstable. Nevertheless, final structures hardly change their geometry when re-relaxed again with different bond centre locations whereas derived quantities (local vibrational modes, energy states) might be more sensitive as these properties depend on the wave functions. Additionally, when comparing total energies for different geometries one has to consider that the cluster might not have the ideal symmetry to represent the point group symmetry of the defect. The error of total energy calculations is up to 0.2 eV, bond lengths are within 2-3 % of the bulk values and local vibrational modes within 10 % of the experimental value. It is only possible to examine some of the large amount of possible configurations for each defect, therefore the lowest energy that is found (local minimum) may not describe the actual defect (global minimum).

2.2 Calculation of donor and acceptor levels

The band gap in Ge is 0.74 eV at 0 K [12] and 0.663 eV at 300 K [13]. For the calculation of the donor or acceptor level, a method is used which was recently described by Resende *et al.* [14]. The donor level with respect to the valence band E_v is the difference between the ionisation energy of the defect and that of bulk Ge. In principle, it is possible to calculate the ionisation energy of the defect I_d by the cluster method if the wave function of the defect is localised within the cluster and does not overlap the surface. As the valence band wave functions are not localised, this does not work for the bulk ionisation energy I_b. Therefore the ionisation energy of a standard defect I_s and the experimental value of its donor level $E(0/+)_s$ will be used to eliminate I_b. The position of the donor level $E(0/+)_d$ is then

$$E(0/+)_d = E(0/+)_s + I_d - I_s \ .$$

For the calculation of the acceptor levels the same method applies but this time with taking the electron affinities A_d and A_s (defect and standard defect respectively). The electron affinity is the work done when moving an electron from infinity to the defect. The acceptor level of the defect $E(-/0)_d$ is then given as

$$E(-/0)_d = E(-/0)_s + A_d - A_s \ .$$

This method leads to very good result. The DFT calculations for determining the donor and acceptor levels are carried out using a spin-polarised calculation. The reference for the electrical levels was taken as Au [13] or Se [15] (Table 1).

	$(-/0)$	$(0/+)$	$(+/++)$
Au	$E_v + 0.15$	$E_v + 0.05$	-
Se	-	$E_c - 0.2688$	$E_v + 0.17$

Table 1: Acceptor and donor energies of Au [13] and Se [15] are given in eV relative to the valence or conduction band edge.

3 Self-interstitials

In the following section, several basic models for the single interstitial are described and the lowest energy geometries for the interstitial and its aggregates in Si and diamond are listed. Finally a detailed discussion of the calculated results for the structures in germanium is given. One of the reasons why interstitials form aggregates is to lower the energy compared to two isolated structures by reducing the number of dangling bonds (unpaired orbitals). The I_4 and I_3 (W-line) structures described below have only fourfold-coordinated atoms and thus have a relatively low energy.

3.1 Models for the single interstitial

Several configurations for the single interstitial were considered as starting arrangements:

- The bond centred interstitial lies in the middle of a bond (Fig. 1). A bond centred cluster would be ideal to reflect the symmetry of the defect which is D_{3d}.

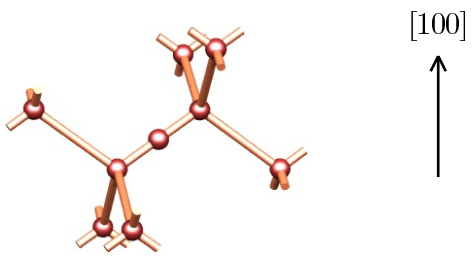

Figure 1: The bond centred interstitial

- The D_{3d} symmetric hexagonal interstitial lies in a hexagonal cage (Fig. 2).

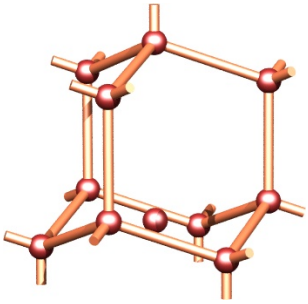

Figure 2: The hexagonal interstitial

- Fig. 3 shows a cluster containing a tetrahedral interstitial which is placed into a tetrahedral cage, as seen on the right. The symmetry of the defect is T_d.

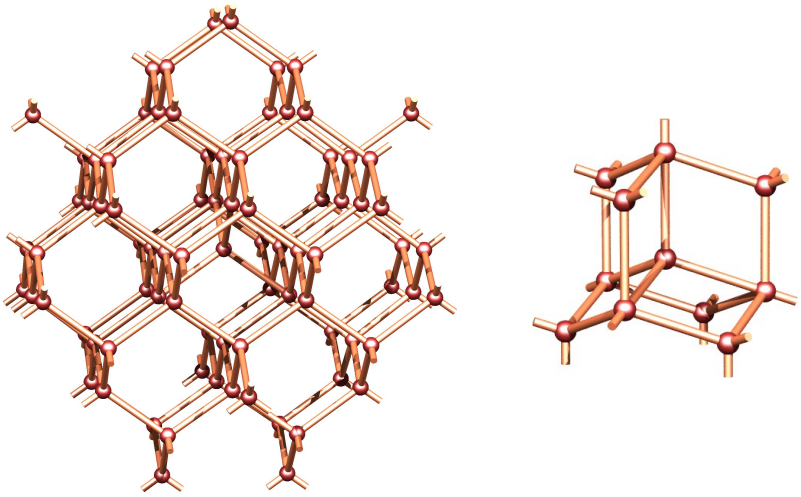

Figure 3: Left: Cluster containing a tetrahedral interstitial. Right: The interstitial is placed into a tetrahedral cage.

- The dumbbell $\langle 100 \rangle$ split-interstitial is constructed by placing an additional atom in the normal unit cell which forms a dumbbell with the centre atom. The dumbbell is aligned along the $\langle 100 \rangle$ direction. The

symmetry of the defect is D_{2d}.

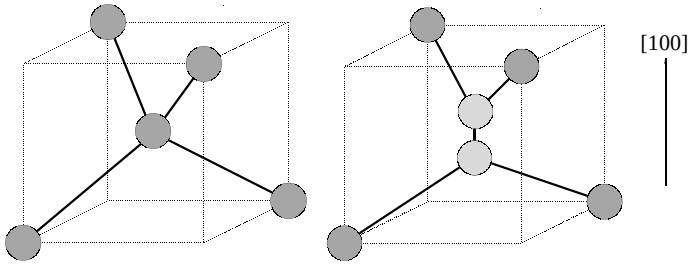

Figure 4: Unit cell and $\langle 100 \rangle$ split-interstitial [16]

- The dumbbell $\langle 110 \rangle$ split-interstitial defect, originally proposed by Bar-Yam and Joannopoulus [17] is mainly spread over four atoms. The upper two atoms are fivefold coordinated. The dumbbell is aligned along the $\langle 110 \rangle$ direction and the defect has C_{2v} symmetry.

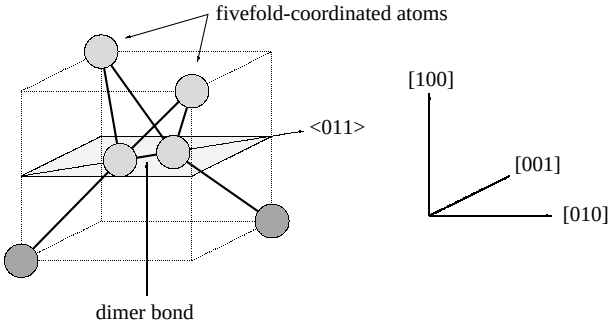

Figure 5: The $\langle 110 \rangle$ split-interstitial

3.2 The self-interstitial and its aggregates in diamond and silicon

The atomic electronic configuration consisting of four sp^3 hybridised covalent bonds leads to the diamond structure where each atom is surrounded by four neighbours in a tetrahedral arrangement. This is the case for silicon, germanium and diamond. However, the bonding of carbon can be both sp^2 (graphite) and sp^3 hybridised (diamond) with similar energies. Therefore one might expect that diamond and Si (or diamond and Ge) show different lowest energy structures which is in fact the case. The question is whether the lowest energy structures of the interstitial aggregates in Ge differ from those in Si. Ge is known to be 'softer' as silicon with a slightly larger lattice constant (bond length Ge: 2.450 Å, Si: 2.352 Å, C (diamond): 1.544 Å, C (graphite): 1.426 Å). For Si it was found experimentally that there exist 'magic numbers' in the early annealing stages for interstitial aggregates (*e.g.* I_4 and I_8) by estimating their formation energies [18]. It is believed that these structures transform to the extended defects at certain temperatures. In the following a brief summary of the types of interstitial defects found both theoretically and experimentally in diamond and silicon is given.

3.2.1 Single interstitial I_1

Chadi calculated in 1992 by *ab initio* methods [19] that the dumbbell $\langle 110 \rangle$ split-interstitial (Fig. 5) is the lowest energy structure in Si which was confirmed by many other authors, in fact all *ab initio* calculations I am aware of yielded this result.

For diamond it was found that the $\langle 110 \rangle$ is not stable. The ground state structure was identified to be the dumbbell $\langle 100 \rangle$ split-interstitial (Fig. 4). Recent EPR experiments have pointed out that the R2 centre in diamond is a $\langle 100 \rangle$-oriented split-interstitial [5].

3.2.2 Di-interstitial I_2

In diamond, the spin $S = 1$ EPR centre labelled R1 has been identified with the di-interstitial [3]. It has C_{2h} symmetry and is built up of two $\langle 100 \rangle$ split-interstitials at nearest neighbour (NN) sites (Fig. 6).

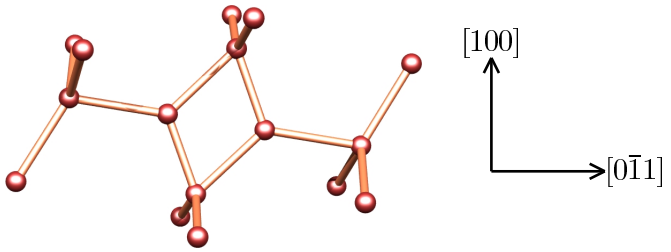

Figure 6: The NN di-interstitial in diamond

For Si, Kim *et al.* [20] proposed a model for the di-interstitial in silicon which has C_{1h} symmetry (Fig. 7) to account for the P6 centre which can be observed in ion, neutron or proton implanted silicon. However, Kim's model is completely inconsistent to experiment because the P6 centre has C_2 symmetry at low temperature and D_2 at room temperature [21]. Although through hyperfine structure, symmetry and stress alignment measurements the P6 centre is linked to the di-interstitial, the lowest energy C_2 structure of I_2 is still not determined.

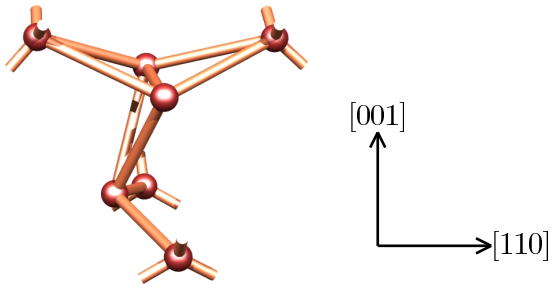

Figure 7: The C_{1h} di-interstitial model for Si proposed by Kim.

Coomer *et al.* [22] found another low energy model for the I_2 in Si which also has C_{1h} symmetry (Fig. 8). The two interstitials share one lattice site

with an atom by forming a triangle in the centre of the defect. The two-atom dumbbell $\overline{\mathrm{AA}}$ consisting of the front bar of this triangle is aligned along the $\langle 011 \rangle$-direction.

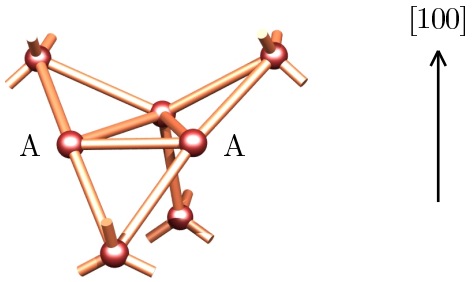

Figure 8: The C_{1h} di-interstitial model for Si found by Coomer.

3.2.3 Tri-interstitial I_3

The EPR O3 centre in diamond [4] was recently identified by Coomer *et al.* with the tri-interstitial which is built up of three $\langle 100 \rangle$ split-interstitials at next-nearest-neighbour sites [23] (Fig. 9). The defect has C_2 symmetry and two threefold-coordinated atoms. Adding a further $\langle 100 \rangle$ split-interstitial leads to a tetra-interstitial model described below (Fig. 11).

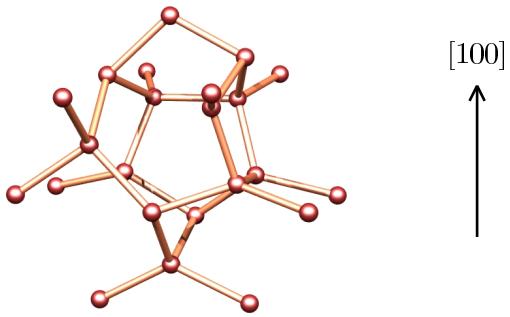

Figure 9: The tri-interstitial model responsible for the O3 centre in diamond.

Coomer *et al.* [22] proposed a C_{3v} tri-interstitial model for the W-optical centre (also labelled I_1; here I_1 originates from a photoluminescence notation and has nothing to do with a single interstitial) which is observed in neutron, electron, proton or heavy ion irradiated, annealed silicon and has trigonal

symmetry. The W centre is a sharp zero-phonon line at 1.018 eV observed in absorption and luminescence. This model is constructed by inserting each additional atom in the middle of three parallel bonds which surround a tetrahedral interstitial site. The three interstitials reconstruct to form a three-atom ring at the centre of the defect and thus all atoms are fourfold coordinated. Coomer *et al.* [22] found that this structure is a three-atom section of a [110] interstitial-chain which is a basic building block of the {311} planar defects which occur after high temperature annealing of irradiated silicon.

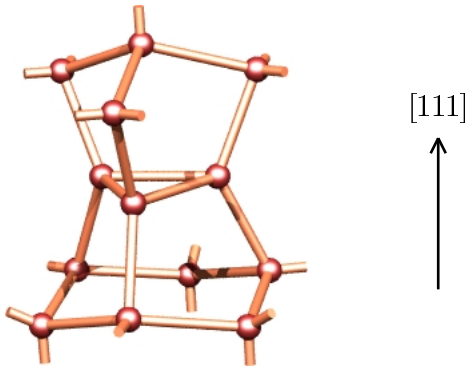

Figure 10: The tri-interstitial model proposed for the W-optical centre in Si.

3.2.4 Tetra-interstitial I_4

Originally, the I_4 model was proposed by Humble [24] as a possible building block for extended defects observed in irradiated diamond. Subsequently Arai *et al.* [16] suggested it as a model for the I_4 in silicon. It consists of four $\langle 100 \rangle$ split-interstitials at next nearest neighbour sites. All atoms are fourfold coordinated and all angles and bond lengths are close to that of bulk Ge (Fig. 11). Therefore it is not surprising that this model is found to be particularly stable. The symmetry is D_{2d} and the I_4 in the positive charge state accounts for the B3 EPR centre in Si [25]. This $S = 1/2$ centre is detected in boron doped, neutron irradiated and heat-treated silicon [26,

	Diamond	Silicon
I_1	EPR R2 centre	
I_2	EPR R1 centre	EPR P6 centre
I_3	EPR O3 centre	optical W centre
I_4		EPR B3 centre

Table 2: The centres in diamond and silicon identified with I_n.

27]. The centre of the defect is vacant. Whereas Arai thought I_4 to be electrically inactive, Coomer *et al.* [25] calculated a single donor (0/+) at around $E_v + 0.2$ eV. This is very close to the $E_v + 0.29$ eV hole trap which is correlated to B3 and was observed in deep level transient spectroscopy (DLTS) studies [28]. Deep levels lie within the cluster and can trap carriers whereas shallow levels located close to the conduction or valence band are extended over a radius of 100 Å which is bigger than the cluster. No other levels were calculated to lie within the band gap. Due to its structure, the I_4 cannot be regarded as a building block for {311} defects but may account as the basis for {001} aggregates in Ge. Table 2 summarises the current knowledge of experimental observed centres that are assigned to the self-interstitial or aggregates of it in silicon and diamond.

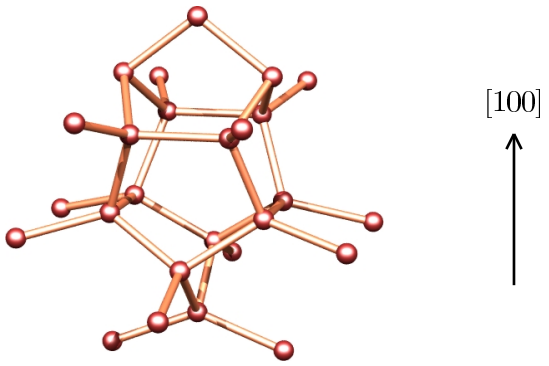

Figure 11: The tetra-interstitial model proposed by Arai for Si.

3.3 The self-interstitial and its aggregates in germanium

In the following section, the results are presented for the self-interstitial and its aggregates in germanium.

3.3.1 Ge single interstitial I_1

For the single interstitial I_1 two types of clusters were used. The atom centred cluster consisted of 132 atoms ($Ge_{72}H_{50}$), the tetrahedral interstitial site centred cluster of 305 atoms ($Ge_{185}H_{120}$). The pure clusters ($Ge_{71}H_{50}$, $Ge_{184}H_{120}$) were first relaxed allowing all atoms to move. The interstitial was placed into the centre of the cluster. The relaxations were carried out with the positions of the surface H atoms fixed. Various symmetry constraints were applied on the relaxations. When a geometry was found as stable, the symmetry constraints were removed by perturbing the positions of the atoms by not more than 0.5 a.u. (1 atomic unit = 0.529 Å).

In agreement with previous *ab initio* calculations by Budde *et al.* [7] and Janotti *et al.* [29], the ⟨110⟩ split-interstitial (Fig. 5 and 12) was found to be the lowest energy configuration in the neutral charge state. The ⟨100⟩ split-interstitial (Fig. 4) which is the ground state configuration of diamond was found to be 0.9 eV higher in energy, although it was only stable under a D_{2d} symmetry constraint. An unconstrained relaxation of the perturbed ⟨100⟩ configuration led to the ⟨110⟩ split-interstitial. The length of the dimer bond along ⟨110⟩ was obtained to be 2.44 Å and the four bonds between these dimer atoms (A) and the fivefold-coordinated atoms (B) are 2.57 Å as indicated in Fig. 12. The ideal bulk bond length is 2.450 Å. The AIMPRO results for the ⟨110⟩ in Si are 2.25 Å (dimer) and 2.45 Å respectively (ideal bulk bond length: 2.352 Å). These two calculations were carried out in an atom centred cluster (298 atoms, $Ge_{182}H_{116}$ and $Si_{182}H_{116}$). These values are compared in Table 3 with the results of da Silva *et al.* [30] and Clark and Ackland [31] who used a different *ab initio* approach (super-cell). It is difficult to draw conclusions from these values about significant differences

	Ge	Ge (da Silva)	Si	Si (Clark)
ideal bulk bond length	2.450	2.450	2.352	2.352
$\overline{\text{AA}}$: dimer bond along $\langle 110 \rangle$	2.44	2.60	2.25	2.40
$\overline{\text{AB}}$	2.57	2.60	2.45	2.46
ratio $\overline{\text{AA}}$ / ideal	0.996	1.061	0.957	1.020
ratio $\overline{\text{AB}}$ / ideal	1.049	1.061	1.042	1.046
ratio $\overline{\text{AA}}$ / $\overline{\text{AB}}$	0.949	1.000	0.918	0.976

Table 3: A comparison of the bond lengths (in Å) and their ratios in Ge and Si obtained with cluster (AIMPRO) and super-cell codes (da Silva, Clark).

of the $\langle 110 \rangle$ geometries in Si and Ge. The Si and Ge results differ in the dimer bond length, probably because of different computational methods. Due to the fact that all bond lengths are 2.60 Å, da Silva *et al.* [30] conclude that the $\langle 110 \rangle$ defect in Ge involves four rather than two atoms as in Si and call it a kite-defect. Table 3 and preliminary AIMPRO super-cell results for Si and Ge which reproduced da Silva's values suggest that the picture of a distinct kite-defect which should be different to the Si $\langle 110 \rangle$-split is probably not justified.

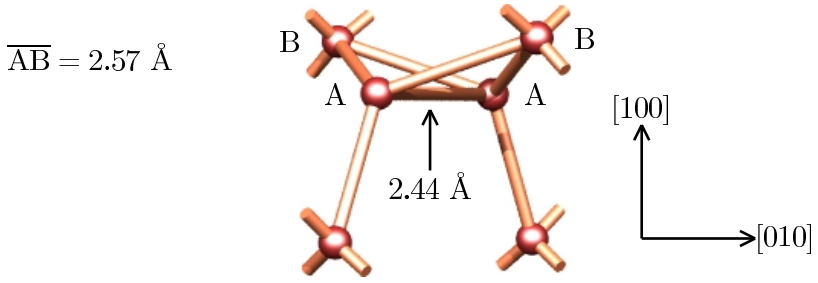

Figure 12: The relaxed $\langle 110 \rangle$ split-interstitial configuration in Ge obtained with the AIMPRO cluster code. The fivefold-coordinated atoms are indicated by the letter B, the dimer atoms by A.

The T_d constrained tetrahedral interstitial (Fig. 3) was found to be 1.1 eV higher in energy (da Silva: 0.9 eV [30]) and was unstable when relaxed in the atom centred cluster. The hexagonal interstitial (Fig. 2) was found to be meta-stable around 0.2 eV higher in energy in the T_d centred

cluster whereas it was unstable in the atom centred cluster and relaxed into a distorted ⟨100⟩ split-interstitial (Fig. 13) which has C_{1h} symmetry and was found to be 0.3 eV higher in energy. These findings show that it is important to pay attention to the fact that the cluster should be appropriate to the symmetry of the defect in order to gain reliable results. It is advisable to compare the energy differences of the cluster calculations with those obtained with the super-cell method where this problem is eliminated but then defect-defect interactions might play a role when using a small super-cell. The C_{1h} structure is important for a new di-interstitial model which is described in the next section. However, preliminary calculations with the AIMPRO super-cell code suggest that this distorted ⟨100⟩ is not stable. From the C_{1h} structure a C_2 structure can be constructed which has its C_2 axis along [010] but was found to be unstable and relaxed into the ⟨110⟩-split. Da Silva *et al.* [30] found the hexagonal to be 0.65 eV higher in energy implying that the ⟨110⟩ is significantly more stable than in Si (only 0.1 eV higher [32]). Preliminary AIMPRO super-cell results support this and therefore the cluster results for the energy difference of the hexagonal to the ⟨110⟩ may be questioned as they do not represent the symmetry of the hexagonal defect. This might be solved by choosing a hexagonal interstitial site centred cluster. As in Si, the bond centred interstitial (Fig. 1) was found to be unstable and relaxed into the ⟨110⟩ configuration.

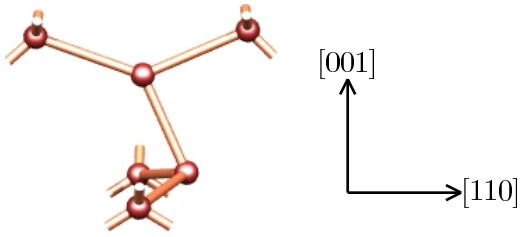

Figure 13: The C_{1h} model which is a distorted ⟨100⟩ split-interstitial.

Haesslein *et al.* [8] identified the mono-vacancy in Ge using perturbed angular correlation (PAC) spectroscopy and DLTS. They also found an-

other type of defect which they tentatively assigned to the self-interstitial (a complex consisting of a Cd atom and an interstitial). PAC spectroscopy utilises radioactive probes, which are incorporated into the systems under consideration. At the decay of a nuclear probe two g-quanta are emitted, whose angular distribution yields information on the local environment of the emitting nuclear probe. The mono-vacancy was identified by the recoil of a neutrino whereas the assignment of the interstitial could only be made by the exclusion of other possibilities. From the trapping behaviour of the Cd atom they could conclude a donor level $(0/+)$ for I_1 lying at 0.04 ± 0.02 eV below the bottom of the conduction band. It is possible that the energetics of the interstitial are affected by the Cd atom. Janotti *et al.* [29] calculated the $(0/+)$ level for the $\langle 110 \rangle$ configuration to be 0.15 eV above the valence band. They questioned the assignments made by Haesslein and use his experimental results to obtain a value of $E_v + 0.1$ eV for $(0/+)$ which is close to their *ab initio* results of $E_v + 0.15$ eV rather than $E_c - 0.04$ eV. A recent publication by da Silva *et al.* [30] calculated the $(0/+)$ level for the $\langle 110 \rangle$ configuration to be 0.07 eV above the valence band, and they suggested that the PAC data should be re-interpreted in terms of a $(0/-)$ level at $E_v + 0.31$ eV which is 0.12 eV below their conduction band and a $(0/+)$ level between 0.11 and 0.16 eV.

The energetics of the ionised interstitial were also examined (Fig. 14). For the 2+ charge state the tetrahedral interstitial was found to be the lowest and the $\langle 110 \rangle$ split was found to be much higher in energy than the $\langle 100 \rangle$.

In the 1+ charge state two different types of a tetrahedral-like were found to be the lowest which are of a similar type as the planar and non-planar self-interstitial suggested by De Souza *et al.* [33]. The two split-interstitials $\langle 110 \rangle$ and $\langle 100 \rangle$ are nearly degenerate in the positive charge state.

In contrast to Ref. [29] no donor level was identified to lie within the band gap for the $\langle 110 \rangle$ whereas for the tetrahedral interstitial a double donor level

Configuration	I_1	I_1/sc	$I_1{}^+$	$I_1{}^+$/sc	$I_1{}^{2+}$	$I_1{}^{2+}$/sc
$\langle 110 \rangle$	0.0	0.0	0.3	0.3	1.4	0.9
hexagonal	0.2	0.6	0.4	0.8	unstable	1.2
distorted $\langle 100 \rangle$	0.3	unstable		unstable		unstable
$\langle 100 \rangle$	(0.9)	1.3	0.2	1.1	0.5	1.1
tetrahedral	(1.1)	0.3	0.0	0.0	0.0	0.0

Table 4: Total energies of the I_1 in the neutral, 1+ and 2+ charge states. Brackets indicate that the defect was only stable when symmetry constrained, 'sc' stands for super-cell calculation where the highest possible point group symmetry was used. These defects could be unstable when no symmetry constraints are applied.

$(+/++)$ close to the conduction band was found. Table 4 shows the energy differences for I_1 in the neutral, 1+ and 2+ charge states and compares the results of the cluster calculations with the preliminary results obtained with the super-cell code (64 atom unit cell). The energies are in eV relative to the ground state.

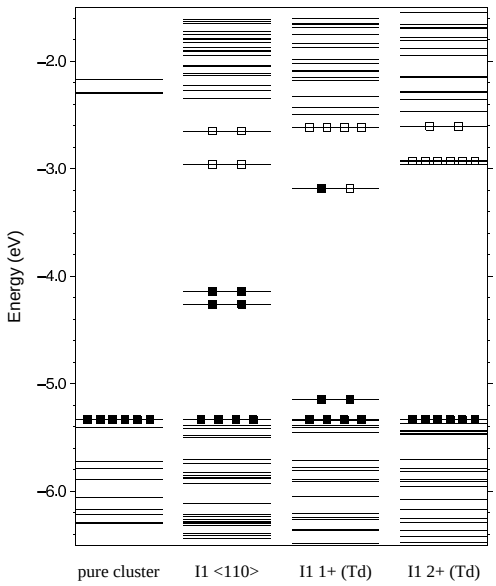

Figure 14: The Kohn-Sham levels of the lowest I_1 structures in the neutral, 1+ and 2+ charge states. The filled (unfilled) boxes represent occupied (unoccupied) states.

3.3.2 Ge di-interstitial I_2

To investigate I_2, an atom centred cluster consisting of 165 atoms was used ($Ge_{89}H_{76}$). For the di-interstitial four competitive ground state structures were found. As described above two of these models were already proposed for Si by Kim (Fig. 7) and Coomer (Fig. 8). The new models (Fig. 15 and 16) have C_2 and C_i symmetry. In experiment it was found that the P6 centre in Si has C_2 symmetry at low temperature with its C_2 axis aligned along the [100] direction [21]. As the structure of I_2 in Si is still not determined, a [100]-oriented C_2 axis for I_2 in Ge would have been likely to be lowest in energy in Si as well. Unfortunately, the axis of the new C_2 model is aligned along [110]. Three out of these four degenerate structures are very similar in terms of bonding and can be transformed into each other by only displacing the central atoms by a small amount. They all have several over-coordinated Ge atoms, and consequently the barrier to reorientation is likely to be small due to a very flat energy surface.

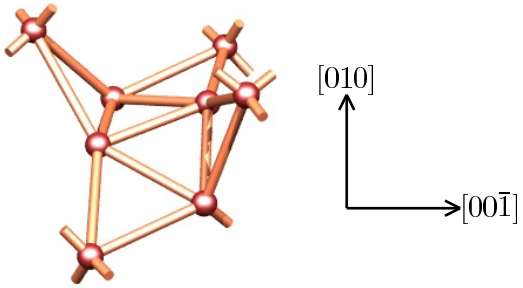

Figure 15: The C_2 di-interstitial model which is very similar to the model found by Coomer. Its C_2 axis is along the [110] direction.

The model that is responsible for the R1 centre in diamond was found to be 0.7 eV higher in energy whereas a similar one (Fig. 16) was found to be nearly as stable as the other three low energy models although the cluster type was not ideal for reflecting the symmetry of the defect. It consists of two distorted $\langle 100 \rangle$ split-interstitials at nearest neighbour sites. This explains the similarity to the di-interstitial model in diamond (Fig. 6) which consists

of two ⟨100⟩ splits at NN sites.

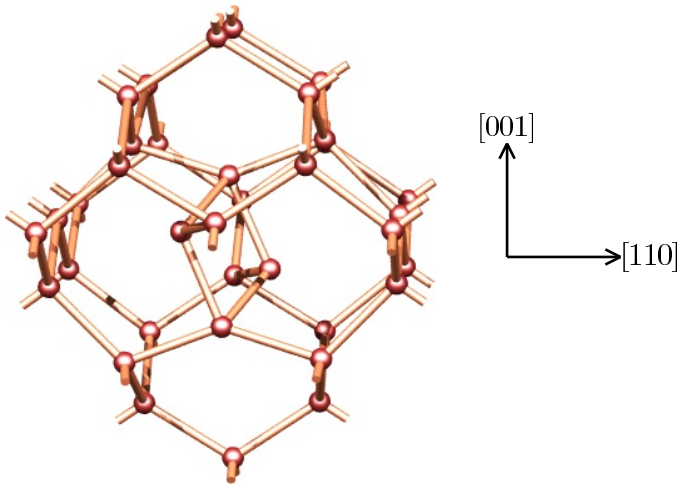

Figure 16: The C_i di-interstitial model which is very similar to the model responsible for the EPR R1 centre in diamond.

Remarkably, this structure has two under-coordinated atoms (threefold coordinated) and their 'dangling bonds' lead to empty states in the band gap that could give rise to an optical centre ('R1like' in Fig. 17). As Si prefers to be over-coordinated whereas diamond prefers under-coordination, it is interesting that Ge has a low energy structure for I_2 containing under-coordinated atoms. However, preliminary super-cell calculations could not reproduce its low energy and yielded 1.0 eV higher in energy than the Coomer and Kim models. Fig. 17 compares the Kohn-Sham levels of the four lowest energy structures. The filled levels of all the low-energy structures are similar. For the Kim model, a single donor level close to the valence band was found. An acceptor level could not be identified. It is expected that the other models would possess similar electrical levels but calculations should still be performed.

Several further models were considered. The configuration formed by two ⟨100⟩-splits at next nearest neighbour (NNN) sites which has two non-bonding p orbitals was found to be stable but 0.6 eV higher in energy. The

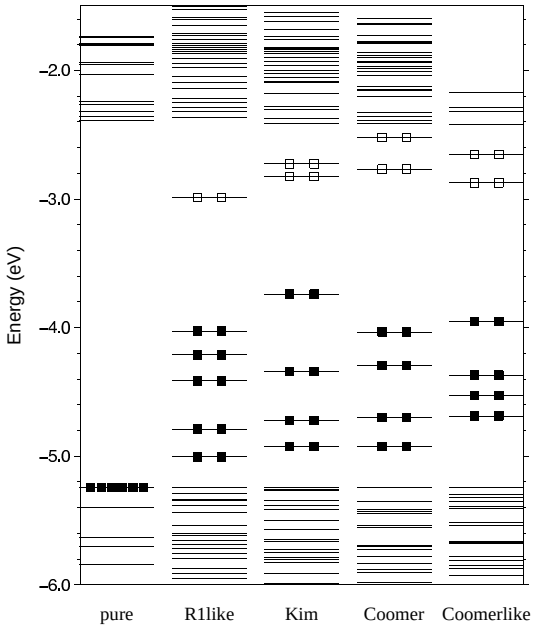

Figure 17: The Kohn-Sham levels of the lowest energy I_2 structures. The model similar to the R1 centre in diamond clearly shows empty states in the band gap due to its under-coordination.

model proposed by Lee [34] was found to be unstable in agreement with previous calculations in Si [22]. Two bond centred interstitials placed on opposite sides of the hexagonal ring relaxed into two five-atom rings 0.5 eV higher in energy.

3.3.3 Ge tri-interstitial I_3

For the tri-interstitial two cluster types were used. The atom centred cluster consisted of 300 atoms ($Ge_{184}H_{116}$) and the tetrahedral interstitial centred one of 307 atoms ($Ge_{187}H_{120}$). Four different configurations were compared:

- The configuration responsible for the O3 centre in diamond (Fig. 9).
- The structure suggested for the W-line in Si (Fig. 10).
- A model proposed by Colombo for I_3 in Si [35] which has T_d symmetry and where four atoms are sharing a single lattice site (Fig. 18).

- The C_{3v} symmetry model suggested by Gharaibeh, Estreicher and Fedders for Si [36] where four atoms are also sharing a single lattice site (Fig. 19).

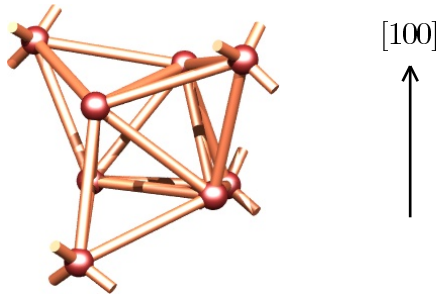

Figure 18: The tri-interstitial model proposed by Colombo for Si.

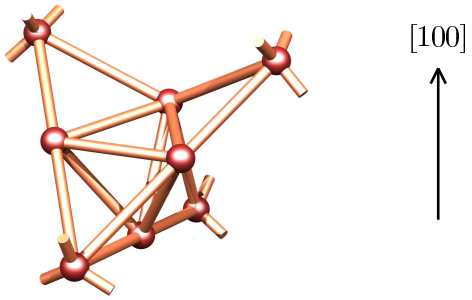

Figure 19: The tri-interstitial model proposed be Gharaibeh *et al.* for Si.

The 300 atom cluster has ideal symmetry to represent the Colombo and Gharaibeh defects whereas the 307 atom cluster is ideal for the two other geometries. The Gharaibeh model was found to be the lowest in energy in the 300 atom cluster. The energies (eV) of these four models are given in Table 5 and are relative to the ground state.

The O3 structure that is lowest in diamond was found to be higher in energy than other models. This was also the case for the I_1 and I_2 diamond ground state models. The Ge I_1 and I_2 results were very similar to the results found for Si. The same calculations were carried out in the 307 atom

Model	Energy	Symmetry constraints
Gharaibeh	0.0	C_{3v}
Colombo	0.2	T_d
W-line	0.9	C_{3v}
O3	1.5	without

Table 5: Total energies of I_3 in the 300 atom cluster (atom centred).

Model	Energy	Symmetry constraints
Colombo	0.0	without
Gharaibeh	0.3	C_{3v} + without
W-line	0.3	C_{3v}
O3	1.6	C_2

Table 6: Total energies of I_3 in the 307 atom cluster (tetrahedral interstitial site centred).

cluster which is ideal for the W-line and O3 models. The outcome looks surprisingly slightly different (Table 6).

It is not clear to determine which structure is the lowest energy. Due to the appropriate symmetry of the smaller cluster, the Gharaibeh model might be tentatively favoured to be the ground state configuration. Future AIMPRO super-cell calculations may probably help to answer this question. Preliminary super-cell results for Si show that the W-line model is not the lowest in energy either. As it is the case in Si, there are empty states in the band gap for the lowest I_3 structure (Fig. 20). This suggests the possibility that they might be detectable via absorption or luminescence processes. The Kohn-Sham levels of the Colombo model are very similar to the Gharaibeh model. I_3 is anticipated to be a donor although an estimate of the position of the level is pending.

3.3.4 Ge tetra-interstitial I_4

For the I_4, a tetrahedral interstitial site centred cluster was used containing 308 atoms ($Ge_{188}H_{120}$). A number of initial configurations were relaxed

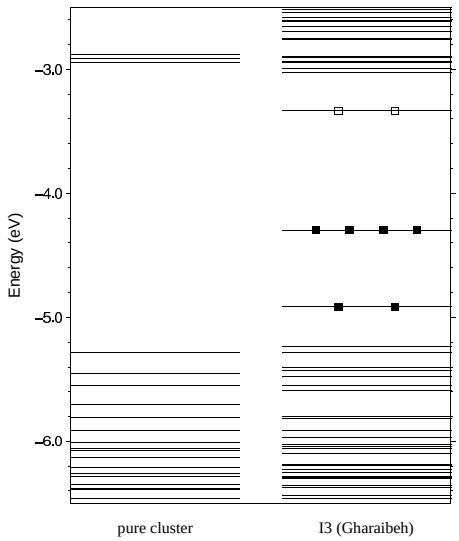

Figure 20: In Ge the I_3 has empty states in the band gap.

consisting of I_3 models with an additional atom but all of them were more than 1.9 eV higher in energy than the model suggested by Arai for Si (Fig. 11). This model was found to be particular stable. Even when all 14 atoms were perturbed significantly, it relaxed back into the lowest energy structure.

The structure which consists of the W-line model (Fig. 10) plus a hexagonal interstitial placed into the hexagonal ring below the triangle was found to be 3.6 eV higher in energy. A model which consists of the W-line plus an interstitial in the centre of the triangle was found to be 6.4 eV higher in energy. A C_{2v} structure involving a pyramid was 2.4 eV and a C_{1h} structure involving eleven triangles was 1.9 eV above the ground state. As in Si it was found that the lowest energy I_4 gives rise to a singlet and a doublet level in the band gap (Fig. 21). It is likely that this defect has a donor level close to the valence band top.

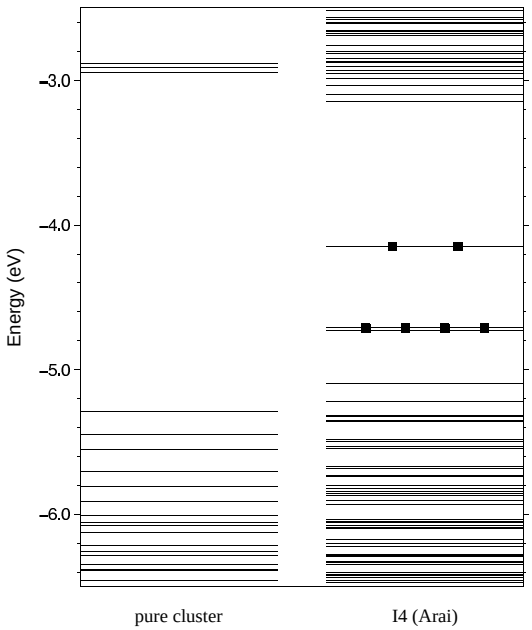

Figure 21: In Ge the band gap has a singlet and a doublet level for the I_4.

4 Conclusions

This work investigated the self-interstitial and its aggregates in germanium. The energetics of the defects are broadly similar to the results found for the corresponding defects in silicon but quite different from diamond. It was confirmed that the $\langle 110 \rangle$ split-interstitial is the ground state structure for the I_1 in the neutral charge state. For the 1+ and 2+ charge states the tetrahedral site interstitial was found to be the lowest in energy, which has potential implications for enhanced interstitial migration under ionising conditions. I_1 is predicted to have a double donor level close to the conduction band in the T_d configuration, but the $\langle 110 \rangle$ is electrically inert. For the I_2 four models were found to be very low in energy, three of them being very similar to each other. It is likely that reorientation between different structures has a low energy barrier. Additionally to Kim's and Coomer's model two new models with C_2 and C_i symmetry respectively were suggested. As in Si, there are empty states in the band gap for the lowest I_3 structure, I_1

and I_2 also have empty levels. This suggests the possibility that they are detectable via absorption or luminescence processes. The I_4 configuration is the same as in Si, also with a doublet and a singlet level in the band gap. All interstitial aggregates that were studied appear to have donor levels close to the valence band top, which could have implications for p-type material.

Future work will concentrate on examining larger aggregates (multi-interstitials I_n) and determining the processes by which the large extended defects are formed by the microscopic interstitial aggregates. To carry this out, larger clusters and molecular dynamics simulations are needed. Hopefully, one will then be able to find the mechanism of transient enhanced diffusion of dopants.

The interstitial aggregates will be examined in various charge states and possible optical centres will be calculated. In germanium, experimental data of structural, vibrational and electrical properties for interstitials and their aggregates need to be obtained to compare with theoretical studies and stimulate further modelling.

5 References

[1] L. Colace, G. Masini, G. Assanto, H.-C. Luan, K. Wada, L.C. Kimerling, *Efficient high-speed near-infrared Ge photodetectors integrated on Si substrates*, Appl. Phys. Lett. **76** (10), 1231 (2000)

[2] G.D. Watkins, J.W. Corbett, Phys. Rev. **138** , A543 (1965)

[3] D.J. Twitchen *et al.*, Phys. Rev. B **54**, 6988 (1996)

[4] D. Hunt *et al.*, to be published

[5] M.E. Newton *et al.*, to appear in Physica B (1999)

[6] S. Takeda, M. Kohyama, K. Ibe, *Interstitial defects on* {113} *in Si and Ge - Line defect configuration incorporated with a self-interstitial atom chain*, Phil. Mag. A **70** (2), 287 (1994)

[7] M. Budde, B. Bech Nielsen, P. Leary, J. Goss, R. Jones, P.R. Briddon, S. Öberg, S.J. Breuer, *Identification of the hydrogen-saturated self-interstitials in silicon and germanium*, Phys. Rev. B **57** (8), 4397 (1998)

[8] H. Haesslein, R. Sielemann, C. Zistl, *Vacancies and Self-Interstitials in Germanium Observed by Perturbed Angular Correlation Spectroscopy*, Phys. Rev. Lett. **80** (12), 2626 (1998)

[9] R. Jones, P.R. Briddon, Chapter 6 in *Identification of Defects in Semiconductors*, Vol. 51A of *Semiconductors and Semimetals*, edited by M. Stavola, Academic Press, Boston (1998)

[10] G.B. Bachelet, D.R. Hamann, M. Schlüter, Phys. Rev. B **26**, 4199 (1982)

[11] P. Hohenberg, W. Kohn, Phys. Rev. B **136**, 864 (1964)

[12] S. M. Sze, *Physics of Semiconductor Devices*, 2nd edition, John Wiley & Sons, New York (1981)

[13] H. Bracht, N.A. Stolwijk, H. Mehrer, *Diffusion and solubility of copper, silver, and gold in germanium*, Phys. Rev. B **43** (18), 14465 (1991)

[14] A. Resende, R. Jones, S. Öberg, P.R. Briddon, *Calculations of Electrical Levels of Deep Centers: Application to Au-H and Ag-H Defects in Si*, Phys. Rev. Lett. **82** (10), 2111 (1999)

[15] C.S. Olsen, J.W. Beeman, K.M. Itoh, J. Farmer, V.I. Ozhogin, E.E. Haller, *Selenium double donors in neutron transmutation doped, isotopically controlled germanium*, Solid State Comm. **108** (11), 895 (1998)

[16] N. Arai, S. Takeda, M. Kohyama, *Self-Interstitial Clustering in Crystalline Silicon*, Phys. Rev. Lett. **78** (22), 4265 (1997)

[17] Y. Bar-Yam, J.D. Joannopoulus, Phys. Rev. Lett. **52**, 1129 (1984)

[18] N.E.B. Cowern, G. Mannino, P.A. Stolk, F. Roozeboom *et al.*, Phys. Rev. Lett. **82**, 4460 (1999)

[19] D.J. Chadi, *Self-interstitial bonding configurations in GaAs and Si*, Phys. Rev. B **46** (15), 9400 (1992)

[20] J. Kim, F. Kirchhoff, W.G. Aulbur, J.W. Wilkins, F.S. Khan, G. Kresse, *Thermally Activated Reorientation of Di-interstitial Defects in Silicon*, Phys. Rev. Lett. **83** (10), 1990 (1999)

[21] Y.H. Lee, N.N. Gerasimenko, J.W. Corbett, Phys. Rev. B **14**, 4506 (1976)

[22] B.J. Coomer, J.P. Goss, R. Jones, S. Öberg, P.R. Briddon, *Interstitial aggregates and a new model for the I_1/W optical centre in silicon*, to appear in Physica B

[23] B.J. Coomer, J.P. Goss, R. Jones, T.D. Shaw, P.R. Briddon, S. Öberg, *Self-interstitial aggregation in diamond*, submitted to Phys. Rev. Lett.

[24] P. Humble, Proc. R. Soc. Lond. A **381**, 65 (1982)

[25] B.J. Coomer, J.P. Goss, R. Jones, S. Öberg, P.R. Briddon, *Identification of self-interstitial aggregates in silicon*, to be published

[26] K.L. Brower, Phys. Rev. B, **14**, 872 (1976)

[27] D.F. Daly, J. Appl. Phys. **42**, 864 (1971)

[28] B.N. Mukashev, A.V. Spitsyn, N. Fukuoka, H. Saito, Jpn. J. Appl. Phys. **21**, 399 (1982)

[29] A. Janotti, R. Baierle, Antônio J.R. da Silva, R. Mota, A. Fazzio, *Electronic and structural properties of vacancy and self-interstitial defects in germanium*, Physica B **273-274**, 575 (1999)

[30] Antônio J.R. da Silva, A. Janotti, A. Fazzio, R.J. Baierle, R. Mota, *Self-Interstitial Defect in Germanium*, to be published

[31] S. Clark, G. Ackland, *Ab initio calculations of the self-interstitial in silicon*, Phys. Rev. B **56** (1), 47 (1997)

[32] J. Zhu, T.D. dela Rubia, L.H. Yang, C. Mailhiot, G.H. Gilmer, Phys. Rev. B, **54**, 4741 (1996) and references therein

[33] M.M. De Souza, C.K. Ngw, M. Shishkin, E.M. Sankara Narayanan, *Planar Self-interstitial in silicon*, Phys. Rev. Lett. **83** (9), 1799 (1999)

[34] Y.H. Lee, *Silicon di-interstitial in ion-implanted silicon*, Appl. Phys. Lett. **73** (8), 1119 (1998)

[35] L. Colombo, *Native defects and their interactions in silicon*, Physica B **273-274**, 458 (1999)

[36] M. Gharaibeh, S.K. Estreicher, P.A. Fedders, *Molecular-dynamics studies of self-interstitial aggregates in Si*, Physica B **273-274**, 532 (1999)